On-Line Dynamic Cable Rating for Underground Cables based on DTS and FEM

Y.C.Liang*[1,2] Y.M.Li[1]

[1]School of Electrical Engineering
Xi'an Jiaotong University
No 28 Xianning West Road, Xi'an
CHINA

*[2]Department of Electrical and Information
Hebei University of Science and Technology
No 70 Yuhua East Road, Shijiazhuang
CHINA

yongchunliang@hotmail.com

Abstract: - The development of surface temperature on-line monitoring techniques for 110kV and above XLPE power cable gives a strong support to power cable load dynamic adjustment. However, the problem is how to determine the conductor temperature from the surface temperature. A technique based on distributed temperature sensing (DTS) and finite element method (FEM) is presented to estimate the soil thermal properties by matching the computed thermal fields to that obtained from measurement and predict the real-time current carrying capacity by iterative method in order to prevent overheat of insulation. Compare with the thermal circuit model, the method based on DTS and FEM is more accuracy.

Key-Words: - Online monitoring，Dynamic cable rating，Distributed temperature sensing， Finite element method, current carrying capacity, Underground cables

1 Introduction

In densely populated areas, electricity is usually transmitted and distributed through buried cables. The main disadvantage of buried installations is to obtain, with sufficient accuracy, the maximum values of current that can flow through the cables in steady states without insulation deterioration.

For modern HV cables, oil-filled paper-insulated cable can be operated at maximum temperature of 85 $°C$ and XLPE insulated cable at a maximum temperature of 90 $°C$. There are several factors determining the current carrying capacity of a specific cable circuit, namely, the cable construction, cable surrounding soil, ambient temperature and sheath-bonding method. Of these factors, the thermal properties of soil are always varying whereas the others are relatively stable.

Because the thermal properties of soil change with time depending on the weather in different seasons and the heating in the cable, the current carrying capacity could change significantly from time to time. Therefore, it is important to determine the dynamic rating of a cable circuit so that its full capacity can be utilized all year around, and it is always a challenge for power system operators to assign adequate power load to underground cables without exceeding their current rating [1-5].

Nowadays more and more power utilities have recognized the importance of thermal condition monitoring of buried cable circuits and installed advance distributed temperature sensing (DTS) systems to monitor cable surface temperature [6-14]. In [1], the cable surface temperature is used to improve the calculation model based on IEC 60287 and McGraph/Neher method. However, analytical method is based on some assumption conditions and can't simulate the real condition. The cable surface temperature is just an indirect indication for the cable insulation thermal states. From the viewpoint of cable operation, cable conductor temperature is the most desired and useful quantity, which directly reflects the cable thermal condition [15].

In [16], the conductor temperature is calculated from cable surface temperature by thermal circuit method. However, dynamic rating systems have a limited numbers of discrete sensors-typically thermocouples-that are placed at representative locations on the cable system. There can be several hotspots in a cable circuit, which act as bottle necks to limit the load-carrying capacity. It is vital for a utility to locate and rectify all hotspots in a cable circuit so that it can be driven to its rating limit comfortably. Unfortunately, the system can do a superb job of dynamically rating the cable-based upon measurements at the wrong location.

The temperature distribution of the most used configurations for buried cables under normal loading conditions is shown in figure 1[17]. For the middle cable, the maximum temperature difference of the cable surface is 0.6 °C. For the outer cable, the maximum temperature difference of the cable surface is 1.3 °C. How to select the correct hot point on the surface of cable is very difficult to calculate the conductor temperature and determine the current carrying capacity. In recent years, numerical methods, such as FEM, have been developed for calculating the temperature distribution of electrical equipment [18] [19]. Compared with the analytical methods, numerical methods not only allow better representation of the mutual heating effects, but also permit more accurate modeling of the region's boundary.

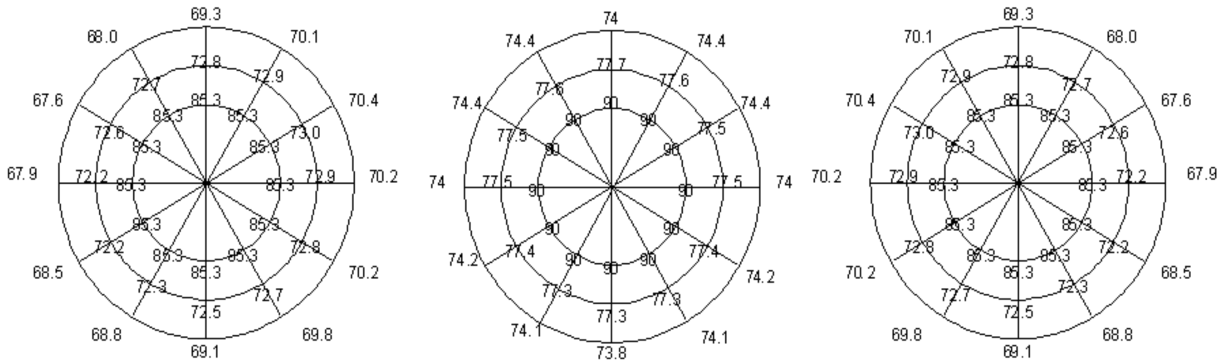

Figure1. A single-loop buried cable's temperature field distribution

In this paper, we use DTS to monitor the surface temperature and estimate the soil thermal properties by FEM and predict the real-time current carrying capacity by iterative method. Compare with the traditional thermal circuit, the position of hot point dose not influence the computational accuracy of the conductor temperature.

2 Overview of the thermal circuit method

A typical single-core power cable is composed of at least four main components, namely, electrical conductor, conductor insulation, sheath, and external covering as shown in figure 2.

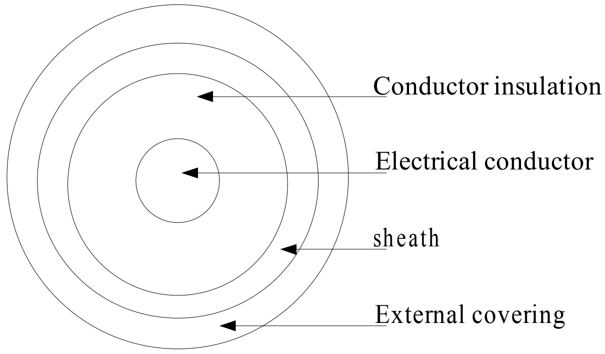

Figure2. The structure of a typical single-core cable

In order to determine heating of underground cable system, the system losses have to be known. The current dependent losses of cables with the solid sheaths can be calculated by finite element method.

For the electric-magnetic field in power cables, the problem can be calculated in two-dimensional Cartesian coordinate system and space charge and displacement current can be neglected. A single-core power cable structure is given in Figure 2. There are two kind of region: metal and others. The Magnetic-vector potential can be described by Lapalace's and Poisson equation differently in these areas.

Magnetic-vector potential equation of cable in different parts under the Coulomb norms is as follows:

Cable conductor region: $\nabla^2 \dot{A}_1 = -\mu_0 \dot{J}_s$, $\dot{J}_s$ is the current density of conductor region.

Cable insulation region: $\nabla^2 \dot{A}_2 = 0$.

Cable sheath region: $\nabla^2 \dot{A}_3 = -\mu_0 \dot{J}_e$, $\dot{J}_e$ is the Eddy current density of metal package region.

Cable external covering region: $\nabla^2 \dot{A}_4 = 0$.

Soil region: $\nabla^2 \dot{A}_5 = 0$.

The continuity equation between different medium is:

$$\dot{A}_i = \dot{A}_j \tag{1}$$

$$\frac{1}{\mu_i}\nabla\cdot\dot{A}_i = \frac{1}{\mu_j}\nabla\cdot\dot{A}_j \tag{2}$$

$$\frac{1}{\mu_1}\nabla\times\dot{A}_1\times n_{12} = \frac{1}{\mu_2}\nabla\times\dot{A}_2\times n_{12} \tag{3}$$

$$i, j = 1,2,3,4,5$$

where i and j represent finite element neighboring region.

Magnetic vector potential can be calculated using FEM [20]. The eddy current in cable conductor and metal package can be calculated by magnetic vector potential as follow:

$$\dot{J}_e = -j\omega\gamma_3\dot{A}_3 \tag{4}$$

where $\dot{J}_e$ represents the current density in metal package; $\dot{A}_3$ represents the magnetic vector potential of metal package region.

Then the conductor electromagnetic loss can be calculated as follow:

$$\begin{aligned} W_c &= \gamma_1^{-1}\int(\dot{J}_s+\dot{J}_e)^2\,dV \\ &= \gamma_1^{-1}\sum(\dot{J}_{s(i)}+\dot{J}_{e(i)})^2\,2\pi r_i S_i \\ &= \gamma_1^{-1}\sum[(\dot{J}_{s(i)}-j\omega\gamma_3\dot{A}_{3,i})^2\,2\pi r_i S_i] \end{aligned} \tag{5}$$

where W_c represents the losses in the conductor; γ_1 represents the conductor conductivity; r_i represents the distance from the center to the axis of each unit; S_i represents the unit area.

Then the sheath electromagnetic loss can be calculated as follow:

$$\begin{aligned} W_s &= \gamma_3^{-1}\int\dot{J}_e^{\,2}\,dV \\ &= \gamma_3^{-1}\sum J_{e(i)}^{\,2}\,2\pi r_i S_i \\ &= \gamma_3^{-1}\sum[(\omega\gamma_3 A_{3,i})^2\,2\pi r_i S_i] \end{aligned} \tag{6}$$

where W_s represents the eddy current loss in the sheath; γ_3 represents the sheath conductivity.

The calculation of the dielectric losses is considered as a rather straightforward task, and details can be found by standard Neher/McGraph and IEC 60287 procedures. Dielectric loss of per unit length in each phase can be calculated as follow:

$$W_d = \omega\cdot c\cdot U_0^2\cdot tg\delta \tag{7}$$

where $\omega = 2\pi f$; $c = \dfrac{\varepsilon}{18\ln\left(\dfrac{D}{d_e}\right)\times 10^{-9}}$, the capacitance in per unit length cable ; $tg\delta$, the insulation loss factor in power system and working temperature; U_0 , the phase voltage ; ε , the dielectric coefficient of insulation material; D , the insulation diameter; d_c , the conductor diameter.

After the losses in the cable is known, the conductor temperature and the current carrying capacity can be calculated by the thermal circuit method based on the standard Neher/McGraph and IEC 60287 procedures, with the further de-rating for potential hot spots, as shown in figure 3.

Now, many power utilities installed advanced DTS systems to monitoring the cable surface temperature θ_w. When current flow through cable is known, the conductor temperature can be calculated as follow.

$$\theta_c = \theta_w + (W_c + \tfrac{1}{2}W_d)\cdot(R_{Tj}+R_{Tw}) + (W_s + \tfrac{1}{2}W_d)\cdot RT_2 \tag{8}$$

where θ_c is the conductor temperature, RT_1 thermal resistance of the conductor insulation, and RT_2 thermal resistance of the external covering.

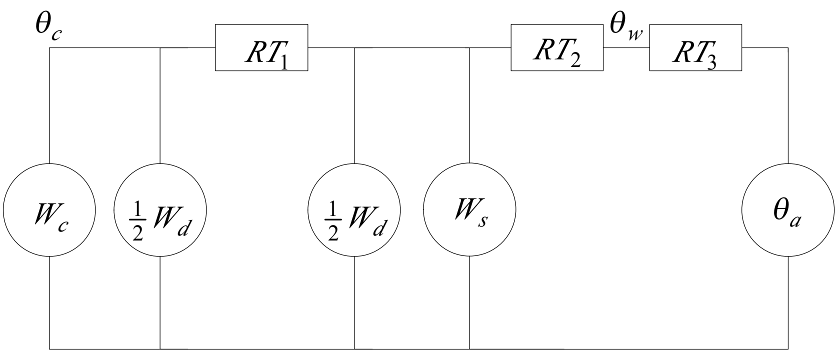

Figure3. The thermal circuit model

The difficult problem in the thermal circuit method is how to determine the surface temperature. Different surface temperature may result in different conductor temperature. But the surface temperature is not an isotherm as shown in Figure 1. With the development of the number of power cables, the surface temperature is more disperse and it is more difficult to determine the correct surface temperature to result correct conductor temperature. Otherwise, because the soil thermal conductivity is highly dependent on moisture content of soil, thermal resistance RT_3 is dynamic and the current carrying capacity calculated by the traditional thermal circuit model as shown in Figure 3 may be not accurate.

3 Principle

3.1Finite element formulation

One of the most used configurations for buried cables consists of three individual cables at the same level with a typical separation between them of one cable diameter as shown in Figure 4. These cables are usually buried directly in the earth or in a backfill material such as concrete or sand. The analysis presented in this paper is based on the following assumptions:

a.The cable system is infinitely long, so that the problem becomes a two-dimensional one.
b. Steady-state conditions exist.
c. All materials have constant thermal properties.
d. The ambient air is stationary.

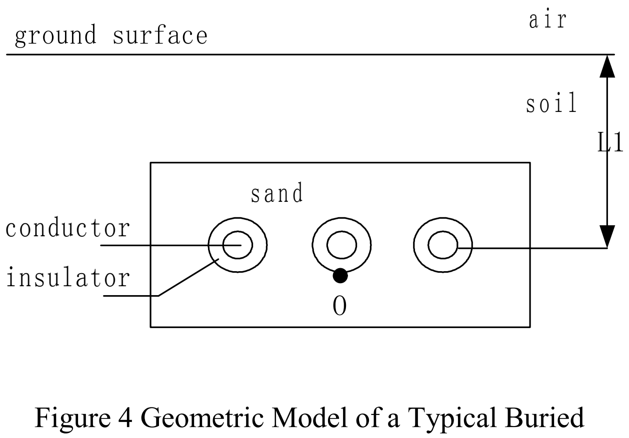

Figure 4 Geometric Model of a Typical Buried Cable Installation

Based on the above assumptions, if the system cross-section lies on the x-y plane, the associated steady-state heat conduction equation for a two-dimensional buried cable system, as shown in Figure 4, can be described as

$$\lambda(\frac{\partial^2 T}{\partial x^2}+\frac{\partial^2 T}{\partial y^2}) = -q \tag{9}$$

where λ is the thermal conductivity $\left(W/\left(m^2\cdot{}^\circ C\right)\right)$, T is the unknown temperature, q is the heat sources generated by cables.

Equation (9) is subjected to the following boundary conditions:

a. In the soil which is far enough away from the cables, both to the sides and underneath, temperature is not affected by the cables' presence. In the areas far enough away underneath the cables, a temperature isotherm is considered to be equal to the deep soil temperature (Ts).In the areas far enough away to the sides from the cables, calorific flow is:

$$\lambda\frac{\partial T}{\partial l}=0 \tag{10}$$

b. At the separation surface between soil and air, convection losses are considered, which means that temperature at this surface is obtained by taking into account Newton's law:

$$Q_1 = h(T - Ta) \tag{11}$$

where h is the convective heat transfer coefficient （ $W/m^2\cdot{}^\circ C)$ ）, T is the temperature at the surface, and Ta is the air temperature.

c. In the separation between the different materials of the cable, between the surface of the cables and the surrounding medium, and between the different materials surrounding the cables, calorific flow continuity is fulfilled at the separation surface:

$$\lambda_1\frac{\partial T}{\partial l}=\lambda_2\frac{\partial T}{\partial l} \tag{12}$$

where l is the normal to the separation surface, and λ_1 and λ_2 represent the thermal conductivity of medium 1 and medium 2, respectively. Likewise, the temperature in both materials at the border points must be the same.

The finite element modeling of equations is obtained by using weak Galerkin's procedure and performs over all the elements [21-22].

$$\frac{\partial J_e}{\partial T_l} = \iint_e [\lambda(\frac{\partial W_l}{\partial x}\frac{\partial T}{\partial x} + \frac{\partial W_l}{\partial y}\frac{\partial T}{\partial y})]dxdy \tag{13}$$

$$\frac{\partial J_e}{\partial T_l} = \iint_e [\lambda(\frac{\partial W_l}{\partial x}\frac{\partial T}{\partial x} + \frac{\partial W_l}{\partial y}\frac{\partial T}{\partial y})]dxdy \tag{14}$$

$$\frac{\partial J_e}{\partial T_l} = \iint_e [\lambda(\frac{\partial W_l}{\partial x}\frac{\partial T}{\partial x} + \frac{\partial W_l}{\partial y}\frac{\partial T}{\partial y})]dxdy + \int_{jm} \alpha W_l (T - T_f) ds \tag{15}$$

The temperatures of every node can be described by equations (16).

$$\begin{bmatrix} k_{11} k_{12} \cdots k_{1n} \\ k_{21} k_{22} \cdots k_{2n} \\ \vdots \\ k_{n1} k_{n2} \cdots k_{nn} \end{bmatrix} \begin{bmatrix} T_1 \\ T_2 \\ \vdots \\ T_n \end{bmatrix} = \begin{bmatrix} P_1 \\ P_2 \\ \vdots \\ P_n \end{bmatrix} \tag{16}$$

Where, k_{ij} and P_i are given by solution of equation (13), (14) and (15). T_i are the temperature of nodes. They are variables desired to solve. $i = 1 \sim n$, $j = 1 \sim n$. n is the number of dissecting node.

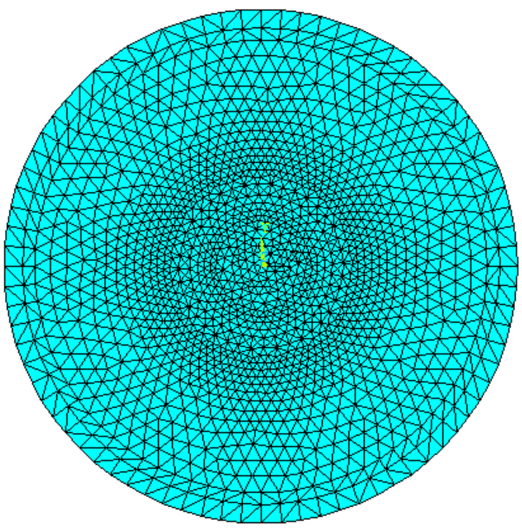

Figure 5 Discretised cable domain: triangular meshes

Discretizing the field domain is usually the most tedious work during implement of FEM. Triangular elements are used in forming the network modeling the cable and surrounding environment. Figure 5 shows the discretised cable domain.

3.2Estimation of soil thermal properties

Once the cable construction, installation, sheath bonding method, cable load and the ambient temperature are determined, the temperature distribution only depends on the thermal properties of the surrounding soil. The thermal properties of soil are always varying. Our site soil test shows that soil thermal conductivity is highly dependent on the moisture content. Under unfavourable conditions, heat flux from the cable entering the soil may cause significant migration of moisture away from the cable. A dried-out zone may develop around the cable, in which the thermal conductivity is reduced by a factor of three or more over the conductivity of the bulk. This in turn may cause an abrupt rise in temperature of the cable sheath and conductor which may lead to damage of cable insulation. How to determine the thermal properties of soil is very difficult using FEM to calculate the thermal field too.

On the middle cable of Figure 3, a DTS optic fiber is installed at point O. Suppose the temperature at surface point "O" is measured with DTS and the soil is taken as a homogeneous thermal medium, the conductor temperature and the effective thermal conductivity of soil can be calculated based on the FEM under the uniqueness theorem of the thermal field.

The temperature at point "O" calculated by FEM is denoted by T_F. The temperature at surface point "O" measured with DTS is denoted by T_m. In this study, the effective thermal properties of soil are determined by minimizing the following objective function.

$$F = \sqrt{\left(T_F - T_m\right)^2} \tag{17}$$

Here, we use subtense truncation approach to calculate the effective thermal conductivity of soil. The literate equation of the subtense truncation approach is equation (18). $T_F(k)$ is the temperature at point "O" calculated by FEM. λ is the effective thermal conductivity of soil. $k+1$ is the next step result, k is the temporary step result, $k-1$ is the last step result.

$$\lambda(k+1) = \lambda(k) + \frac{(T_m - T_F(k)) \cdot (\lambda(k) - \lambda(k-1))}{T_F(k) - T_F(k-1)} \quad (18)$$

The iteration process is terminated if the following condition is satisfied:

The objective F is not greater than 0.1 $°C$.

3.3Prediction of the current carrying capacity

The effective thermal conductivity of soil was adjusted until the calculated temperature was the same as the measured temperature, and the conductor temperature was calculated. A current carrying capacity was calculated until the conductor temperature is equal to 90 $°C$ (XLPE power cable) for those conditions by iterative method. The literate equation of the subtense truncation approach is equation (19). $T_C(k)$ is the conductor temperature calculated by FEM. I is the thermal conductivity of soil. $k+1$ is the next result, k is the temporary result, $k-1$ is the last result.

$$I(k+1) = I(k) + \frac{(90 - T_C(k)) \cdot (I(k) - I(k-1))}{T_C(k) - T_C(k-1)} \quad (19)$$

It is important to note that temperature in a cable system at any time are a function of loading at that time plus the loading for the last week or so because of the very long thermal time constant of the cable/earth system. For example, a cable that has been operating at 700 amperes constantly for 200 hours will be much hotter than a cable that has been operating at 100 amperes for the last 190 hours, then 700 amperes the last ten hours.

So, the current carrying capacity should be calculated for different times, using expected changes in ambient earth temperature and backfill and soil thermal conductivity at those times by the subtense truncation approach.

4 Test and Results

4.1 Method verify

In order to verify the effective the method presented in this paper, we use three buried heat pipes to verify the method as shown in Figure 6

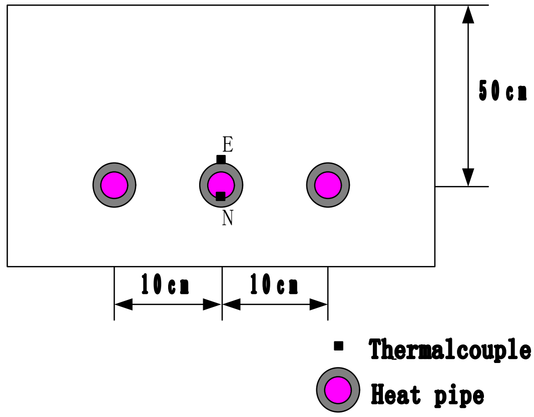

Figure 6 Test model of heat pipe

Three buried heat pipes covered with rubber are placed horizontally at 0.5 m depth and separated 0.1m between the pipe centers. The length of heat pipe is 2.5m and the radius is 0.006m. The thickness of rubber is 0.004m. The thermal conductivity of soil and rubber are 1.664 $W/(m^2 \cdot °C)$ and 0.25 $W/(m^2 \cdot °C)$. The temperature of air is 28 $°C$.

When the power of heat pipe is 92W, the temperature of point "N" after 10 days is 96 $°C$ and the temperature of point "E" after 10 days is 83 $°C$. Using the method presented in this paper, the temperature of point "E" is 82.93 $°C$ and the temperature of point "N" is 95.78 $°C$. The effective thermal conductivity of soil is 1.19 $W/(m^2 \cdot K)$. The result shows that the method is effective to calculated the conductor temperature of power cables and predict the current carrying capacity of power cables with highly accuracy.

4.2 Single loop power cables in horizontally

In this section, the thermal circuit method and the method presented in this paper are applied to estimate the conductor temperatures of single loop underground cables. In order to describe the disperse of the surface temperatures, we measured four point temperature on the surface of cable as shown in figure 7.

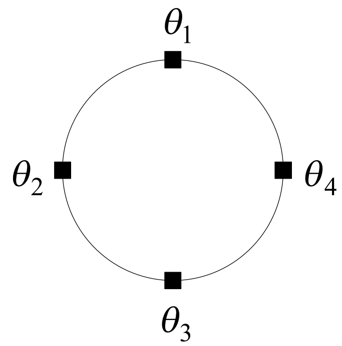

Figure7. The positions of the four points on the cable surface

Three 800mm^2 110kV YJLW02 cables are placed horizontally at 0.7m depth and separated 0.2m between the cable centers. A 35℃ ambient temperature is specified. The current supplying the cables is 500A. When the sheaths are bonded at both ends, the losses in the conductors of different phases are

5.6919 W/5.6989 W/5.6929 W

The losses in the sheaths of different phases are

9.601 W/10.0839 W/13.5855 W

The dielectric losses are 0.69 W.

The ambient thermal conductivity of soil is

$$\lambda_{soil} = 1W/(m^2 \cdot °C)$$

The thermal resistivity of insulation and external covering are

$$3.5\ W/(m^2 \cdot K)$$
$$6\ W/(m^2 \cdot K)$$

The thermal resistance of insulation and external covering are

$$R_{Tj} = 0.4334$$
$$R_{Tw} = 0.0708$$

For the middle cable, the four point temperatures on the surface and the cable conductor temperatures resulted from the cable surface temperature in (8) are shown in table 1. From different surface temperature, the conductor temperature is different. The maximum difference is 0.5 $°C$.

The effective thermal conductivity of soil calculated by FEM and iteration method is 0.7333 $W/(m^2 \cdot °C)$ and the conductor temperature calculated by FEM is 65.13℃. The result by FEM and iteration method is more accuracy. By iteration method, the current carrying capability of single loop power cables placed horizontally with sheath bonded at both ends is 597A at this time.

Table 1The cable surface temperature and the cable conductor temperature

Cable structure	Temperature ($°C$)			
	T_1	T_2	T_3	T_4
Cable surface	61.3	61.6	61.4	61.8
Cable core	65.05	65.35	65.15	65.55

4.2 Three loop power cables in horizontally

In this section, the thermal circuit method and the method presented in this paper are applied to estimate the conductor temperatures of three loop underground cables. Nine 800mm^2 110kV YJLW02 cables are placed horizontally at 0.7m depth and separated 0.1m between the cable centers. The ambient temperature and the thermal conductivity of all thermal medium is the same as above. The current supplying the cables is 500A.

When the sheaths are bonded at both ends, the losses in the conductors of different loop and phase are

Loop1:5.7314 W/5.2976 W/5.7611 W
Loop2:5.7566 W/5.7567 W/5.7587 W
Loop3:5.7541 W/5.7670 W/5.7376 W

The losses in the sheaths of different loop and phase are

Loop1:6.0379 W/6.7763 W/5.7846 W
Loop2:5.7045 W/5.7231 W/5.6367 W
Loop3:6.1392 W/4.7133 W/11.5221 W.

Table 2 shows the surface temperatures of every cable.

For different loop, the current carrying capacity depends on the hottest cable. Table 3 shows the cable conductor temperatures from different surface points by thermal circuit method. The maximum difference for phase C2 is 1.7 $°C$. The maximum difference for phase B2 is 1.2 $°C$. The maximum difference for phase A3 is 1.5 $°C$. With the increase of the number of the power cables, the difference of the cable surface temperature is more disperse and it is more difficult to determine the correct surface hot point to calculate the correct conductor temperature by thermal circuit method.

The effective thermal conductivity of soil calculated by the method presented in this paper is

0.773 $W/(m^2 \cdot °C)$. Table 4 shows the cable conductor temperatures using FEM.

Table 2 The cable surface temperatures of three loop underground cables placed in horizontally

Point	Temperature ($°C$)								
	A1	B1	C1	A2	B2	C2	A3	B3	C3
T_1	70.7	75.9	78.8	80.5	81.2	80.9	79.8	77.3	74.2
T_2	70	76	79.5	81.4	82.3	82.2	81.3	79	76.4
T_3	71.1	76.3	79.2	80.9	82.4	81.3	80.2	77.7	74.6
T_4	73	77.8	80.5	81.9	81.6	81.9	80.5	77.9	73.6

Table 3 The conductor temperatures of three loop power cables placed in horizontally using thermal circuit method

Point	Temperature ($°C$)		
	C1	B2	A3
T_1	82.28	84.97	83.29
T_2	82.98	86.07	84.79
T_3	82.68	86.17	83.69
T_4	83.98	85.37	83.99

Table 4 the conductor temperature of three loop power cables placed in horizontally using FEM

Method	Temperature ($°C$)		
	C1	B2	A3
Fem	82.8	85.09	83.7

By iteration method, the current carrying capability of three loop power cables placed horizontally with sheath bonded at both ends is 459A at this time.

4.3 Single loop power cables in triangular

Three 800mm2 110kV YJLW02 cables are placed in triangular at 0.7m depth. A 35℃ ambient temperature is specified. The current supplying the cables is 500A and the sheaths are bonded at one end.

The losses in the conductors of different phases are

5.9337W/5.9604W/5.9511W

The losses in the sheaths of different phases are

1.7407W/1.9506W/1.8698W

Table 5 shows the surface temperatures of every cable. Table 6 shows the conductor temperatures of every cable by thermal circuit method. The maximum difference of phase A is 1.4 $°C$. The maximum difference for phase B is 1.1 $°C$. The maximum difference for phase C is 1.0 $°C$.

The effective thermal conductivity of soil calculated by the method presented in this paper is 0.773 $W/(m^2 \cdot °C)$.

The conductor temperature of phase A is 53.02 $°C$. The conductor temperature of Phase B is 53.17 $°C$. The conductor temperature of Phase C is 53.15 $°C$.

By iteration method, the current carrying capability of single loop power cables placed in triangular with sheath bonded at one end is 763A at this time.

Table 5 The cable surface temperatures of single loop underground cables placed in triangular

Cable	T_1	T_2	T_3	T_4
Phase A	49.2	49.8	50.6	49.8
Phase B	50.4	49.6	49.8	50.7
Phase C	50.4	50.7	49.7	49.6

Table 6 The cable conductor temperatures of single loop underground cables placed in triangular by thermal circuit method

Cable	T_1	T_2	T_3	T_4
Phase A	52.48	53.08	53.88	53.08
Phase B	53.7	52.9	53.1	54
Phase C	53.69	53.99	52.99	52.89

5 Discussion

Table 1 and table 2 show that the difference of the surface temperature increases with the increase of the number of power cables. Table 1 and table 5 show that the difference of the surface temperature of the power cables placed in triangular is larger than the power cables placed in horizontally. Table 1, table 3 and table 6 show that it is difficult to select the correct surface hot point to calculate the correct conductor temperature. It means that the accuracy of the conductor temperature calculated by thermal circuit method highly dependent on the selection of the hot point of the cable surface. It may give a worst result.

The method based on DTS and FEM can improve the defect. When we know the temperature and the position of the hot point on the cable surface, we can calculate the conductor temperature with high accuracy. At the same time, we can predict the effective thermal conductivity of soil and calculate the current carrying capacity of the power cables by iterative method.

6 Conclusion

DTS systems have been installed by numerous power utilities to monitor in real time the cable surface temperature. To make full use of advanced DTS, a technique based on FEM and surface temperature of cable has been developed to calculate the cable conductor temperature and predict the current carrying capability. The computational results show that the conductor temperature can be determined more accurately. This technique will be useful for the future development of an online dynamic rating system for the underground cables based on DTS.

References:

[1] G.J.Anders, J.M.Braun, S.Ressetto and D.Casselman, Real Time Monitoring System for 230 kV Cables in Tunnels. *IEEE PES Transmission and Distribution Conference and Exposition*, *V*ol.3, 2003, pp. 886-891

[2] Dale A. Douglass and Abdel-Aty Edris, Real-time Monitoring Dynamic Thermal Rating of Power Transmission Circuit, *IEEE Transactions on Power Delivery*, Vol.11, No.3, 1996, pp.1407-1418

[3] Steven P.Walldorf, John S.Engelhardt and Frank J.Hoppe, The Use of Real-time Monitoring and Dynamic Ratings for Power Delivery Systems and the Implications for Dielectric Materials, *IEEE Electric Insulation Magzine,* Vol.15, No.5, 1999, pp.28-33

[4] S.Nakamura, S.Morooka and K.Kawasaki, Conductor Temperature Monitoring System in Underground Power Transmission XLPE Cable Joints, *IEEE Transactions on Power Delivery,* Vol.4, No.4, 1992, pp.688-1697

[5] Q.Su, H.J.Li, K.C.Tan, Hotspot Location and Mitigation for Underground Power Cables, I*EE Proceedings of Generation, Transmission and Distribution*, Vol.152, 2005, pp.934-938

[6] H.J.Li, Estimation of Thermal Parameters and Prediction of Temperature Rise in Crane Power Cables, *IEE Proceeding of Generation, Transmission and Distribution*, Vol.151, 2004, pp.355-360

[7] Gunes Yillmaz, Sait Eser Karlik, A Distributed Optical Fiber Sensor for Temperature Detection in Power Cables, *Sensors and Actuators A*, Vol.125, 2006, pp.148-155

[8] John Downes, CEng, H Y Leung, Distributed Temperature Sensing Worldwide Power Circuit Monitoring Applications, *2004 International Conference on Power System Technology –POWERCON 2004*, pp.1804-1809

[9] V.Dubickas and H.Edin, On-line Time Domain Reflectometry Measurements of Temperature Variations of an XLPE Power Cable, *2006 Annual Report Conference on Electrical Insulation Dielectric Phenomena*, pp.47-50

[10] J. H. Zhao, H. Y. Yuan and W. C. Fan, Surface temperature field based online diagnoses study for electric cable's conductor temperature, *Proceedings of the CSEE,* Vol.1,1999,pp.52-55

[11] Z. W. Gao, X. F. Wei and Q. G. Chen, 2005 Research on forecast and alarm system of ampacity on-line for power cable, *Heilongjiang Electric Power*, Vol.2, 2005, pp.96-99,107

[12] Geoff Nokes, Optimizing Power Transmission and Distribution Networks using Optical Fiber Distributed Temperature Sensing System, *Power Engineering Journal*, Vol.13, 1999, pp.291-296

[13] Vasileiou.D K-E, Agoris.D, Pyrgioti.E, A Review on the Application of Fiber Optics on High Voltage Lines, *WSEAS Transactions on Circuits and Systems*, Vol.3, No.5, 2004, pp.1192-1196

[14] Jay A.Williams, John S.Cooper, Thomas J.Rodenbaugh, et al, Increasing Cable Rating by Distributed Fiber Optic Temperature Monitoring and Ampacity Analysis, *IEEE Transmission and Distribution Conference,* Vol.1, 1999, pp.128-134

[15] H.J.Li, Estimation of Soil Thermal Parameters from Surface Temperature of Underground Cables and Prediction of Cable Rating, *IEE Generation Transmission and Distribution*, Vol.152, No. 6, 2005, pp.849-854

[16] Shun-Hsien Huang, Wei-Jen Lee, Ming-Tse Kuo, An Online Dynamic Cable Rating System for an Industrial Power Plant in the Restructured Electric Market, *IEEE Transactions on Industry Application*, Vol.43, 2007, pp.1449-1458

[17] Carlos Garrido, Antonio F.Otero and Jose Cidras, Theoretical Model to Calculate Steady-State and Transient Ampacity and Temperature in Buried Cables, *IEEE Transactions on Power Delivery*, Vol.3, 2003, pp.667-678

[18] C.C.Hwang, J.J.Chang, H.Y.Chen, Calcualtion of Ampacities for Cables in Trays using Finite Elements, *Electric Power Systems Research*, Vol.54, 2000, pp.75-81

[19] Sharifian Attar.S, Yagoub.MCE, Mohammadi.F, Simulation of Electro-thermal Effects in Device and Circuit, WSEAS Transations on Circuit and Systems, Vol.5, No.7, 2006, pp.926-930(FEM)

[20] D.Labridis, V.Hatziathanassiou, Finite Element Computation of Field, Forces and Inductances in Underground SF6 Insulated Cables using a Coupled Magneto-Thermal Formulation, *IEEE Trans.Magn,* Vol.30,1994, pp.1407-1415

[21] G.J.Anders, M.Caaban, N.Bedard, et al, New Approach to Ampacity Evaluation of Cables in Ducts using Finite Element Technique, *IEEE Transactions on Power Delivery*, vol. PWDR-2, 1987, pp.969-975

[22] J.Nahman, M.Tanaskovic, Determination of the Current Carrying Capacity of Cables using the Finite Element Method, *Electric Power Systems Research*, Vol.61, 2002, pp.109-117